Synthesis and ligand properties of chelating bis(N-heterocyclic carbene)-stabilized bis(phosphinidenes)‡

Jan-Erik Siewert,[a] Braulio M. Puerta Lombardi,[b] Nora Janssen,[a] Roland Roesler,[b] Christian Hering-Junghans*[a]*

‡Dedicated to Douglas W. Stephan on the occasion of his 70th birthday.

[a] M.Sc. Jan-Erik Siewert, Dr. Nora Janssen, Dr. Christian Hering-Junghans
Leibniz Institut für Katalyse e.V. (LIKAT)
A.-Einstein-Str. 29a, 18059 Rostock (Germany)
E-mail: christian.hering-junghans@catalysis.de

[b] Braulio M. Puerta Lombardi, Prof. Roland Roesler
Department of Chemistry, University of Calgary
2500 University Drive NW, Calgary, AB, T2N 1N4 (Canada)
E-mail: roesler@ucalgary.ca

Supporting information for this article is available. These contain all relevant experimental and computational details.

Abstract: N-heterocyclic carbene-phosphinidene adducts (NHPs) are an emerging class of ligands with proven binding ability for main group and transition elements. They can be considered as inversely polarized phosphaalkenes with electron-rich P atoms possessing two lone pairs of electrons, which render them interesting platforms for the formation of multi-metallic complexes. We describe herein a modular, high-yielding synthesis of bis(NHP)s, starting from alkylidene-bridged bis(NHC)s ($(IMe)\}_2C_nH_{2n}$; n = 1,3) and a triphosphirane (*cyclo*-P_3Dip_3) (Dip = 2,6-*i*$Pr_2C_6H_3$) as phosphinidene transfer reagents. The coordination chemistry of [$\{DipP(IMe)\}_2CH_2$], **1**, was studied in detail, and the complexes [**1**·$FeBr_2$] and [**1**·Rh(cod)]Cl were prepared, showing that the ligand has a flexible bite-angle ranging between 86-106°. [**1**·Rh(cod)]Cl was converted into the corresponding dicarbonyl complex [**1**·$Rh(CO)_2$]Cl, with an average value for the CO stretching frequency of 2029 cm^{-1}, which indicates a strongly donating ligand, when compared to related bis(NHC) rhodium complexes. The

binding ability of the remaining two phosphorus lone pairs was demonstrated via addition of $AuCl(SMe_2)$, which generated the hetero-trimetallic complex [**1**·$(AuCl)_2$·Rh(cod)]Cl. Moreover, [**1**·Rh(cod)]X (X^- = Cl, B(3,5-CF_3-$C_6H_3)_4$) were tested in the catalytic hydrogenation of the α,β-unsaturated esters methyl-*Z*-α-acetamidocinnamate (MAC) and dimethyl itaconate ($ItMe_2$), revealing that the chloride complex was inactive, while the BAr^F-complex demonstrated moderate activity, lower than that of analogous complexes incorporating classical diphosphines such as DiPAMP. In addition, [**1**·Rh(cod)]Cl was shown to be moderately air- and moisture stable, slowly decomposing to the corresponding NHC-stabilized bisdioxophosphorane, which was independently synthesized by treating the free ligand with dry O_2.

Introduction

N-heterocyclic carbene-phosphinidenes (NHPs, Scheme 1, **III**) of the general form (NHC)PR are closely related to phosphaalkenes (Scheme 1, **I**), albeit with an inverse polarization or "umpolung" (Scheme 1, **II**)[1] that renders the phosphorus atom highly nucleophilic, while formally holding two lone pairs of electrons (**II** and **III**).[2] Although the zwitterionic resonance **II** (Scheme 1) best describes the electronic situation of NHPs, the term N-heterocyclic carbene-phosphinidene adduct has gained wide acceptance in the chemistry community and will be used throughout the manuscript. The closely related C-amino and C-diamino-substituted phosphaalkenes have been first described in the 1980s and their chemistry has been comprehensively reviewed.[3]

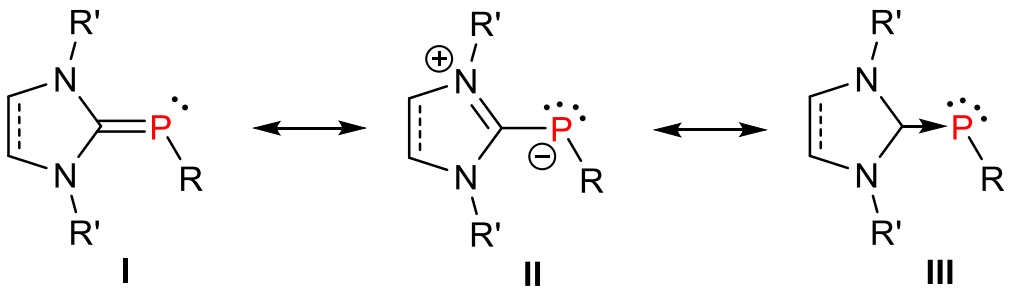

Scheme 1. Resonance forms of NHPs.

NHC-phosphinidene adducts have been explored as ligands in transition metal chemistry, and it was shown that either one or two metal centers can be coordinated at the P atom.[4] Four major pathways for the synthesis of NHC-stabilized aryl-phosphinidenes of the type (NHC)PAr have been devised (Scheme 2): 1. Treatment of $PhPH_2$ with a free NHC in a 1:2 ratio afforded (NHC)PPh, with the concomitant formation of $(NHC)H_2$,[5] a pathway that was also shown to be catalysed by $[M\{N(SiMe_3)_2\}_2]$ (M = Fe, Co).[6] 2. Using $ArPCl_2$, free NHCs and either Mg-powder, KC_8, or an excess of NHC as reductants,[7] allowed the generation of a large variety of (NHC)PAr species. The ^{31}P NMR shift in these compounds has been used to assess the π-accepting properties of the respective NHCs.[8] 3. The first NHC-phosphinidene adduct, $(IMe_4)PPh$ ($IMe_4 = (MeCNMe)_2C$:), was accessed by treatment of the phosphinidene oligomer *cyclo*-$(PPh)_5$ with IMe_4 in a 1:5 ratio.[9]

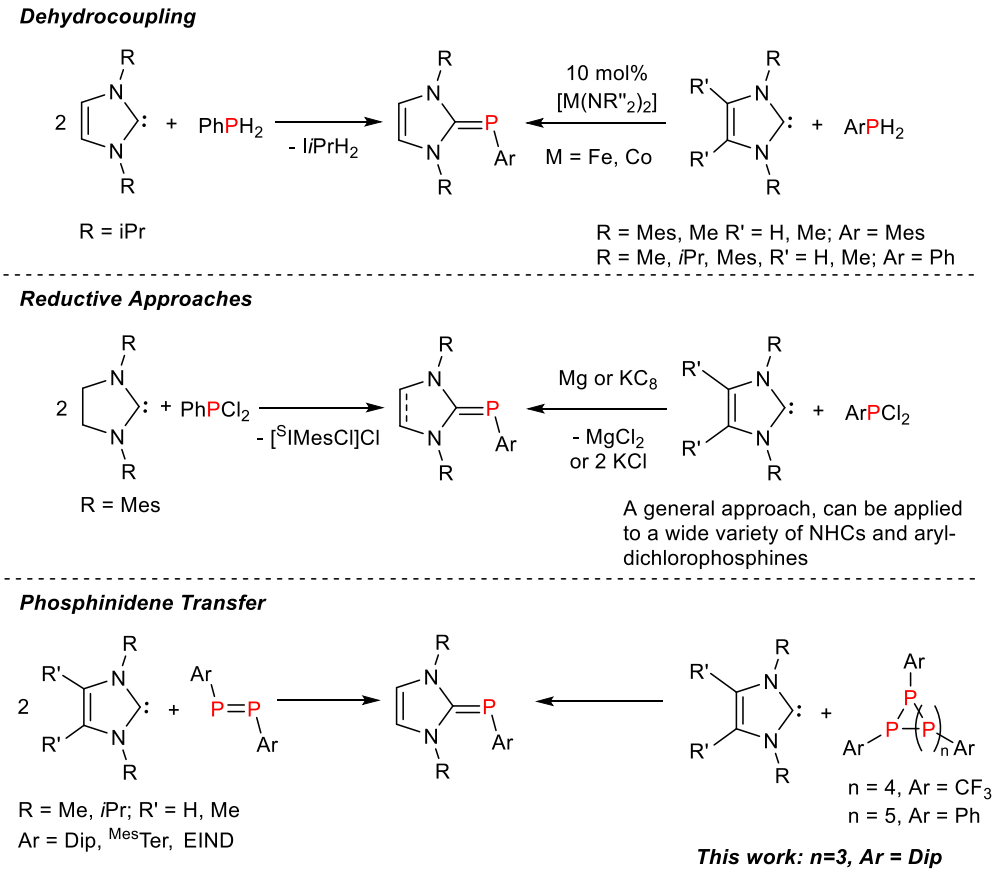

Scheme 2. Synthetic approaches towards NHC phosphinidene-adducts.

This strategy can be generalized and a variety of diphosphenes,[10] or *cyclo*-oligophosphanes *cyclo*-$(PR)_n$ (n = 3,4,5)[11] can be converted into the corresponding (NHC)PR species by treatment with the free phosphinidenes in a 1:n ratio. 4. Our group has recently shown that phosphanylidenephosphoranes of the type ArP(PMe_3) reacted cleanly with NHCs to give a wide range of (NHC)PAr adducts in a Lewis base substitution reaction.[12] Moreover, a variety of different approaches have been used to access the NHC-adducts of the parent phosphinidene PH.[13]

In contrast to the growing number of simple (NHC)PR adducts, the number of chelating bis(NHC-phosphinidene) adducts (or bis(NHP)s) is limited to two examples. Driess and Hadlington were the first to report such species, which were obtained by treatment of the diphosphine Xant-$(PH_2)_2$ with four equivalents of I*i*Pr_2 at 100 °C in toluene, to give Xant-(P{I*i*Pr_2})$_2$ (**A**, XantP_2; Scheme 3, top) accompanied by the formation of I*i*Pr_2H_2.[14] The coordination chemistry of **A** was probed by the addition of ZnI_2 and $FeCl_2$, giving the corresponding pseudotetrahedral, chelating [XantP_2]EX_2 complexes (Scheme 3, top right). With $GeCl_2$·dioxane and $SnBr_2$, the formation of germylium- and stannyliumylidene salts, respectively, was demonstrated. When **A** was treated with CuCl, the cluster compound [(XantP_2)$_2$$Cu_3Cl_2$]Cl was obtained (Scheme 3, top left), in which three of the P atoms are bridging two copper centres, demonstrating that both phosphorus lone pairs can be engaged in coordination.

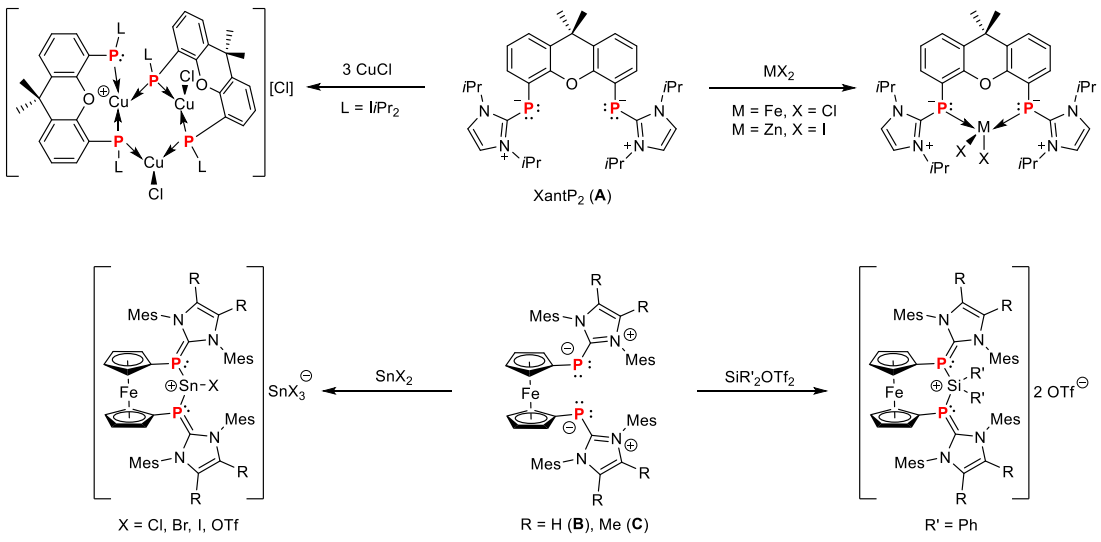

Scheme 3. Reported bis(NHP)s (**A**, top; **B**, **C**, bottom) and their coordination chemistry.

Inoue and co-workers reported that the treatment of 1,1′-bis(dichlorophosphine)ferrocene (1,1′-$(Cl_2P)_2$-Fc) with two equivalents of IMes or ^{Me}IMes, respectively, and direct dechlorination with four equivalents of sodium naphtalenide afforded the corresponding ferrocenyl-bridged bis(NHP)s 1,1′-(^{R}IMesP)$_2$-Fc (R = H (**B**), R = Me (**C**)) (Scheme 3, bottom).[15] Akin to **A**, **B** and **C** were shown to yield stannyliumylidene species in the reaction with SnX_2 (Cl, Br, I, OTf) (Scheme 3, bottom left). Furthermore, [{1,1′-(^{R}IMesP)$_2$-Fc}SnCl][$SnCl_3$] was shown to be capable of transferring the $[SnCl]^+$ fragment onto a bis(N-heterocyclic imine) ligand, bis(NHI). Moreover, the same group recently showed that Si(IV) dications can be effectively stabilized using **B** in the reaction with bis(triflato)silanes (Scheme 3, bottom right).[16] Inspired by the success of bidentate phosphines such as 1,2-bis(diphenylphosphino)ethane (dppe) and (2,2′-bis(diphenylphosphino)-1,1′-binaphthyl), (BINAP), which have been widely applied in coordination chemistry and homogenous catalysis,[17] we have pursued further development in the area of chelating bis(NHP)s. We hypothesized that the easily available bis(NHC)s[18] and triphosphirane[19] starting materials should be able to provide an inverse approach to chelating bis(NHP)s with respect to existing synthetic methodologies, via a phosphinidene transfer reaction (Scheme 2). This would provide an alternative approach to this emerging class of ligands, expanding the available ligand designs. The outcome of these studies, as well as forays into the coordination chemistry of the resulting bis(NHP)s with rhodium and gold, and preliminary investigations of its suitability as an ancillary ligand in catalysis will be described.

Results and Discussion

Bis(imidazolium) precursors were readily obtained in the reaction of methylimidazole with CH_2Br_2,[20] and $Br(CH_2)_3Br$,[21] respectively. Deprotonation of the bisimidazolium salts with KHMDS in THF at −70 °C in the presence of P_3Dip_3 in a 3:2 ratio afforded the desired bis(NHP)s **1** and **2** (Scheme 4) in 73 % and 82 % yield, respectively, as yellow crystalline solids (Scheme 4).

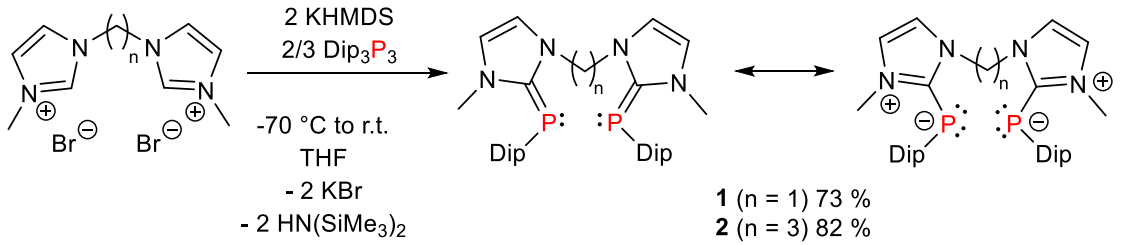

Scheme 4. Synthesis of bis(NHP)s **1** and **2**.

The deprotonation was performed in situ, due to the limited stability of the corresponding free NHCs. The formation of **1** and **2** can be monitored by $^{31}P\{^{1}H\}$ NMR spectroscopy, with singlet resonances at −87.7 and −87.1 ppm, respectively, reflecting product formation. These values fall in the range expected for NHC-phosphinidene adducts (cf. **A** −77.2;[14] **B** −57.0;[15] $(IMe_2)PMes$ −73.8 ppm).[5a, 22] The bridging methylene unit in **1** gives rise to a singlet resonance in the ^{1}H NMR spectrum at 5.88 ppm. Cyclic voltammograms of ligand **1** showed two oxidation events at −0.61 V and −0.36 V *vs*. Fc/Fc^{+}, with the second oxidation being reversible and the first irreversible, as well as an irreversible reduction at −1.53 V (Figures S38, S39). UV-Vis spectroscopy for **1** revealed an absorption at λ_{max} = 389 nm, which was attributed to a HOMO-LUMO transition (p-type lone pair on P to empty p-orbital on C_{NHC}) based on TD-DFT studies (Figure S45). The frontier molecular orbitals indicate that the HOMO and HOMO-1 have significant p-type lone pair character on the P atoms and are delocalized toward the C_{NHC} atoms (Figure S45). The second s-type lone pair on the P atoms is represented by HOMO-2 and HOMO-3, while the LUMO shows main contributions from an empty p-orbital on C_{NHC}, all in line with an inversely polarized phosphaalkene.

X-ray quality crystals of **1** were grown from a saturated *n*-pentane solution at −30 °C.[23] **1** crystallizes in the orthorhombic space group *Aba*2 with four molecules in the unit cell and with half a molecule of **1** in the asymmetric unit. The CH_2-group of **1** is situated on a twofold axis making **1** a C_2-symmetric ligand (Figure 1), akin to classical examples such as BPE,[24] and DiPAMP.[25] The P–C_{NHC} distances (1.773(3) Å) are minimally shorter than those in the two crystallographically confirmed conformers of **A** (cf. 1.790(5)-

1.830(5) Å) and in the same range as in **B** (cf. 1.731(10), 1.808(10) Å) and **C** (cf. 1.7696(18), 1.7704(19) Å), with C–P–C_{NHC} angles in **1** (100.84(13) Å) being similar to those measured in other NHC-phosphinidene adducts.

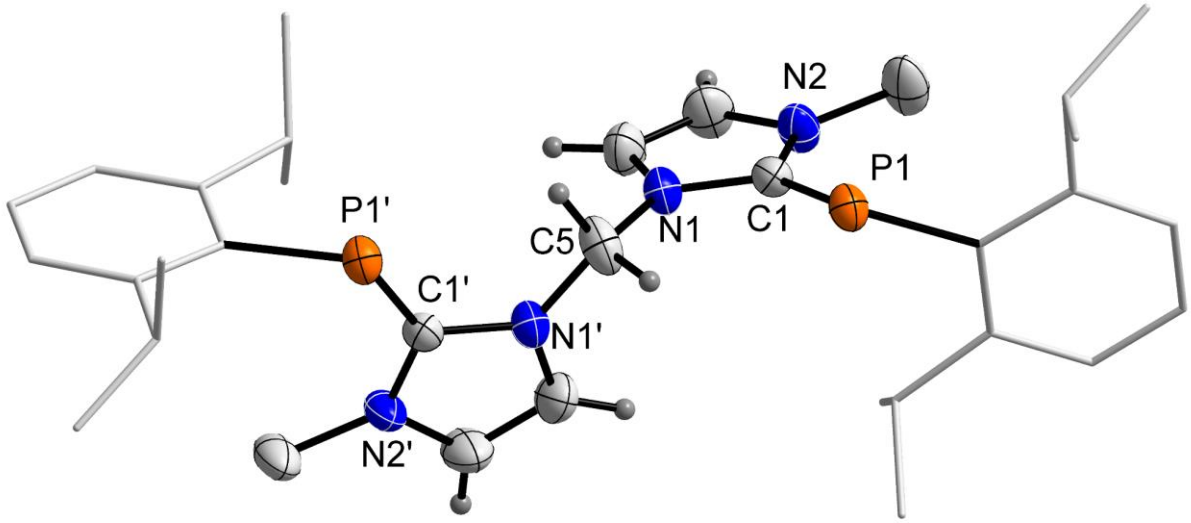

Figure 1. Solid-state structure of **1** with 50% probability thermal ellipsoids and hydrogen atoms on the Dip substituents, which are rendered as wire-frame, omitted for clarity. Selected bond lengths [Å] and angles [°]: P1–C1 1.773(3), P1–C6 1.849(3), C1–N1 1.369(3), C1–N2 1.364(4), N1–C5 1.446(3); C1–P1–C6 100.84(13), N1–C1–P1 123.7(2), N2–C1–P1 132.1(2), N2–C1–N1 103.9(2).

To explore its coordination chemistry, **1** was first combined with $FeBr_2$ in MeCN, giving a red precipitate of [**1**·$FeBr_2$], **3**, which could be recrystallized from MeCN (Scheme 5). No reaction with $FeBr_2$ was apparent when ligand **2** was utilized.

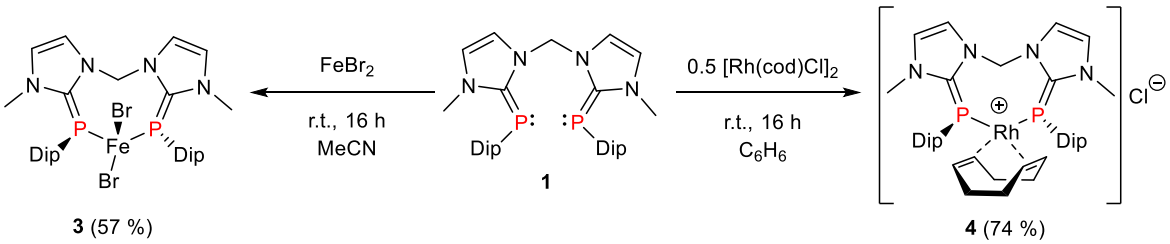

Scheme 5. Synthesis of complexes **3** (left) and **4** (right).

Similar to [{$XantP_2$}·$FeCl_2$], the ^{1}H NMR spectrum of **3** is significantly broadened due the paramagnetic nature of **3** and no resonances were observed in the $^{31}P\{^1H\}$ NMR spectrum. In the solid state, the P–C_{NHC} distances (P1–C1 1.802(3), P2–C6 1.799(3) Å) are elongated compared to the free ligand (cf. 1.773(3) Å), albeit minimally (Figure 2,

left). The Fe(II) center adopts a distorted tetrahedral coordination environment characterised by a τ_4-value of 0.93,[26] while the P atoms are pyramidal, implying engagement of one of the two lone pairs on each P atom. The P–Fe–P angle (106.63(3)°) is similar to that measured in [{XantP$_2$}·FeCl$_2$] (cf. 103.10(5)°).[14] In addition, the bridging CH$_2$-group is oriented in such way that one C–H bond points towards the Fe center, with a nearly linear CH···Fe1–Br2 arrangement and a CH···Fe1 distance indicative of an anagostic interaction.[27] The identity and purity of **3** were further authenticated by elemental analysis and high resolution mass spectrometry (HRMS).

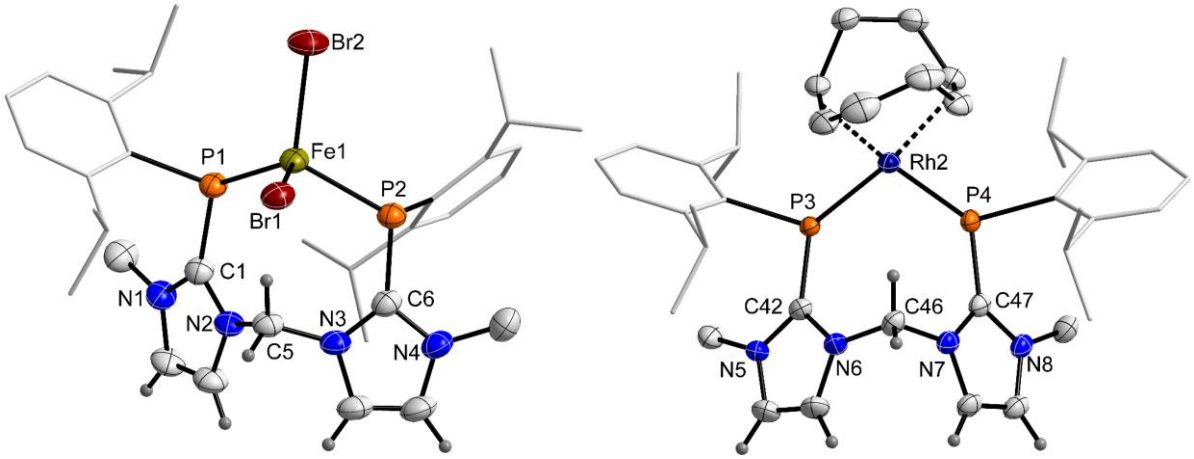

Figure 2. Solid-state structure of **3** (left) with 50% probability thermal ellipsoids and of the cation in **4** (right, one of two independent molecules in the asymmetric unit) with 30% probability thermal ellipsoids. Hydrogen atoms on the Dip substituents, which are rendered as wire-frame, omitted for clarity. Selected bond lengths [Å] and angles [°] of **3**: P1–C1 1.802(3), P2–C6 1.799(3), Fe1–P1 2.3638(9), Fe1–P2 2.4055(9), Fe1–Br1 2.4445(6), Fe1–Br2 2.4326(6); P1–Fe1–P2 106.63(3), P1–Fe1–Br1 118.59(3), P2–Fe1–Br2 110.88(3), N1–C1–N2 104.7(3), N4–C6–N3 104.6(3), C1–P1–Fe1 116.24(10), C6–P2–Fe1 114.94(10). Selected bond lengths [Å] and angles [°] of **4**$^+$, [values in 2nd molecule in the asymmetric unit]: P3–C42 1.803(3) [P1–C1 1.811(3)], P4–C47 1.813(3) [P2–C6 1.794(3)], Rh2–P3 2.3594(7) [Rh1–P1 2.3350(7)], Rh2–P4 2.3496(8) [Rh1–P2 2.3475(8)], Rh2–H46B 2.6123(5) [Rh1–H5B 2.5970(6)]; P3–Rh2–P4 90.91(2) [P1–Rh1–P2 86.76(3)], C42–P3–Rh2 119.36(10) [C1–P1–Rh1 116.61(10)], C47–P4–Rh2 118.73(11) [C6–P2–Rh1 118.76(11)].

When **1** and [Rh(cod)Cl]$_2$ were combined in benzene at room temperature, the complex [**1**·Rh(cod)]Cl, **4**, was isolated upon workup as an orange crystalline solid (Scheme 5). In a $CDCl_3$ solution, **4** displays a doublet resonance in the $^{31}P\{^1H\}$ NMR spectrum at −72.4 ppm ($^1J_{P-Rh}$ = 106.3 Hz). The bound cod-ligand is clearly identified in the ^{1}H NMR

spectrum (−C*H*=C*H*−: 4.26, 3.80 ppm; CH_2: 3 multiplets 2.22−1.70 ppm) and the four doublet and two septet resonances corresponding to the isopropyl groups indicate a time-averaged C_2-symmetric structure in solution. CV studies on **4** show two oxidation events at −0.15 V and 0.28 V *vs.* Fc/Fc^+, with the second one being reversible, and the first being irreversible and coupled to an irreversible reduction at −1.13 (Figure S40), similar to the features observed in free ligand **1**. Using differential pulse voltammetry (DPV), it was shown that the oxidation at −0.15 V is a combination of two redox events (Figure S42).

X-ray quality crystals of **4** were grown by slow diffusion of *n*-hexane into a saturated CH_2Cl_2 solution. The solid-state structure featuring two independent molecules in the asymmetric unit shows an outer-sphere chloride anion and a distorted square planar coordination geometry at the Rh center, with P−C_{NHC} distances (1.801(3)−1.814(4) Å) in the range expected for bis(NHP) metal complexes (Figure 2, right). Similar to **3**, one of the C−H bonds of the bridging NCH_2N moiety is oriented towards Rh (H···Rh 2.6094(5) Å; C···Rh 3.4885(47) Å), in an anagostic interaction.[28] In contrast to agostic interactions, anagostic interactions are characterised by M···H−C distances between 2.3−2.9 Å and rather wide C−H···M angles (110−170°), in line with the parameters observed in the cation of **4** (C46−H···Rh2 148.0(3)°). For example, in the square planar rhodium bis(pyrazolyl)borate complex {BBN(3-R-$pz)_2$}, only a weak Rh···H interaction (H···Rh 2.42(4) Å) was detected, which was interpreted as a three-center, four-electron bond (3c-4e) involving two electrons from the C−H and two from filled Rh d-orbitals, respectively.[29]

Similar weak Rh···H interactions described as 3c-2e bonding were postulated in the related bis(NHC) thione complexes [{(S(IMe))$_2$CH_2}Rh(cod)]X (**D**, X = Cl^-, BF_4^-, PF_6^-).[27] One additional indicator of an anagostic interaction is the significantly deshielded ^{1}H NMR shift of the C−H involved in the interaction, in contrast to an agostic interaction.[30] In **1** the CH_2-moiety is characterised by a singlet resonance at 5.88 ppm in the ^{1}H NMR spectrum, while in complex **4** the signal splits into two doublets at 8.22 and 7.64 ppm with a $^2J_{H-H}$ coupling constant of 13 Hz. This is in contrast to **D**, where a

splitting into an AB spin system is only observed upon cooling to −78 °C.[27] To further authenticate the anagostic nature of this interaction, DFT calculations were performed. To visualize the weak Rh···H contact, an interaction region indicator (IRI) analysis was carried out, which visually reveals both chemical bonds and weak interactions in molecules.[31] It indicated a region of notable attraction between rhodium and the respective hydrogen (turquoise region between both atoms) in line with the presence of an anagostic interaction (Figure 3). This was further corroborated by an Atoms in Molecules (AIM) analysis (Figure S43), showing a bond critical point (BCP) along the Rh···H bond path with a low electron density $\rho(r)$ (0.02) and a small positive value for the Laplacian $\nabla^2\rho(r)$ of 0.05 (Table S8), all in line with recently reported theoretical studies on anagostic interactions.[32]

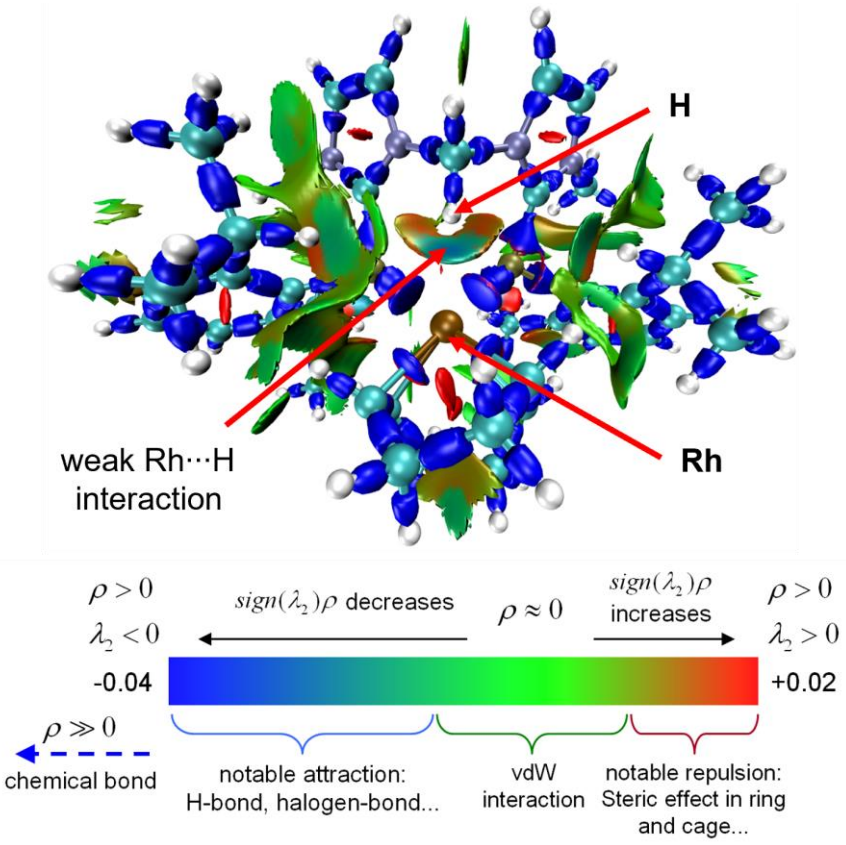

Figure 3. Isosurface plot of IRI=1.0 (right). Notable attractions are indicated by turquoise regions, whereas dark blue areas indicate chemical bonding. Grid spacing for IRI is 0.12 Bohr. Obtained at the PBE0-D3/def2-TZVP//PBE0-def2SVP level of theory. Color bar from Tian et al.[31]

The hydrogenations of methyl-*Z*-α-acetamidocinnamate (MAC) and dimethyl itaconate ($ItMe_2$) with various Rh/Ligand systems are some of the most widely investigated hydrogenations and are often used as benchmark systems to evaluate the performance of novel ligand frameworks.[33] **4** displayed no catalytic activity toward the hydrogenation of MAC and $ItMe_2$, in contrast to other LRhCl species.[34] The complex was, however, stable under one atmosphere of H_2 in MeOD solution at room temperature over a period of 4 h (Figure S35). We thus performed an anion exchange reaction using **4** and $Na[B(3,5\text{-}(CF_3)_2\text{-}C_6H_3)_4]$ ($NaBAr^F$) in CH_2Cl_2, which was accompanied by the formation of a white precipitate presumed to be NaCl. The product [**1**·Rh(cod)][BAr^F] (**5**) was characterized by a $^{31}P\{^1H\}$ NMR resonance at −70.2 ppm ($^1J_{P-Rh}$ = 111.8 Hz) and characteristic ^{11}B and ^{19}F NMR signals corresponding to the $[BAr^F]^-$ anion at −6.6 and −62.8 ppm, respectively. The result was further corroborated by elemental analysis and HRMS studies.

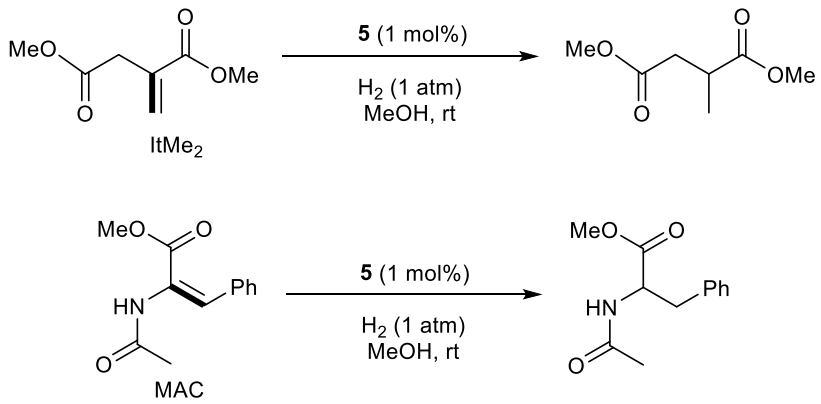

Scheme 6. Synthesis of complexes **3** (left) and **4** (right).

In contrast to **4**, **5** was able to catalyze the hydrogenation of MAC and $ItMe_2$ (Scheme 6). Under standard conditions (1.0 mmol substrate, 0.01 mmol pre-catalyst **5**, 25 °C, 1.01 bar total pressure), a gradual hydrogen consumption was observed (Figures S32-S34) and both reactions were completed after ca. 60 h. For comparison, hydrogenation of MAC and $ItMe_2$ with $[Rh(DiPAMP)(MeOH)_2]BF_4$ was complete after 20 min and 50 min, respectively.[35] It is important to mention that the slow hydrogenation of the COD-ligand results in long induction periods for the catalytic hydrogenation of the prochiral olefins using such systems. For example, if $[Rh(DiPAMP)(cod)]BF_4$ is used

directly for the hydrogenation of MAC (instead of the solvent complex), the reaction time increases from 20 to 160 min.[35] The slow hydrogenation of the COD ligand is reflected in the prominent induction periods in both hydrogenation curves (Figure S34).

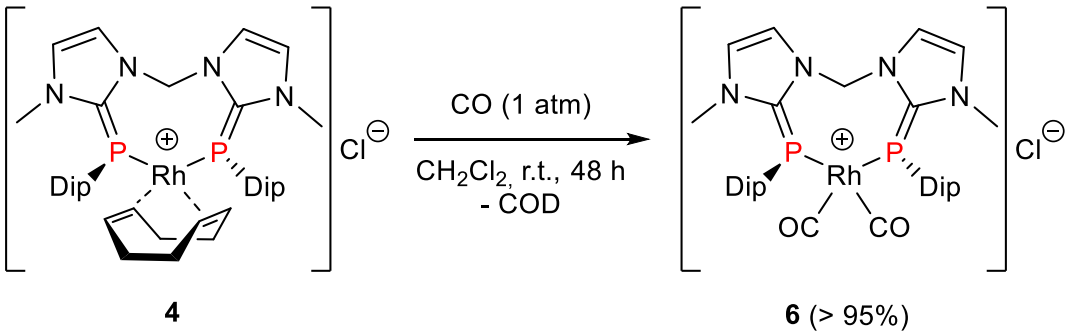

4 **6** (> 95%)

Scheme 7. Synthesis of dicarbonyl complex **6**.

To further explore the properties of ligand **1**, complex **4** was exposed to an atmosphere of CO in a CH_2Cl_2 solution. After stirring at room temperature for 48 h and removal of the solvent, the CO-complex [**1**·$Rh(CO)_2$]Cl, **6**, was obtained as an orange solid in ca. 90 % yield (Scheme 7). Slow diffusion of *n*-hexane into a saturated CH_2Cl_2 solution of **6** afforded crystals suitable for X-ray diffraction experiments. The complex crystallizes in the orthorhombic space group *Pbca* as a CH_2Cl_2 solvate, with one formula unit in the asymmetric unit. To the best of our knowledge, **6** is the only structurally characterized [$LRh(CO)_2$]Cl complex featuring an ionic structure, [**1**·$Rh(CO)_2$]$^+Cl^-$. The Rh(I) center is in a distorted square-planar coordination environment characterized by a τ_4-value of 0.17 (Figure 4).[26] The Rh–P distances (Rh1–P1 2.3742(6), Rh1–P2 2.3902(6) Å) are longer than those measured in **4** (cf. 2.3355(10)-2.3583(10) Å), while the Rh–C_{CO} distances approach those in structurally characterized [{(*R*,*R*)-^{Ph}BPE}$Rh(CO)_2$]BF_4 (cf. 1.879(3), 1.896(3) Å; (*R*,*R*)-^{Ph}BPE = 1,2-bis-[(R,R)-2,5-diphenyl-phospholano]ethane). The C–O distances in **6** (C34–O1 1.142(3), C35–O2 1.131(3) Å) are longer compared to those in [{(*R*,*R*)-^{Ph}BPE}$Rh(CO)_2$]BF_4 (cf. 1.118(3), 1.119(4) Å). Also, elongated (compared to the free ligand) P–C_{NHC} distances (1.819(3), 1.804(3) Å) indicate that π-electron density is removed from the P–C_{NHC} bond. In the $^{13}C\{^1H\}$ NMR spectrum the CO ligands are characterized by a pseudo doublet of triplets at 186.2 ppm. Due to similar $^1J_{Rh-C}$ and $^2J_{Ptrans-C}$ coupling constants (ca. 60 Hz, cf. [(IDipPPh)$RhCl(CO)_2$] $^1J_{Rh-C}$ = 72 Hz for

CO_{cis})[4d] only the $^2J_{Pcis-C}$ (29.0 Hz) could be clearly assigned. The C_{NHC} atom gives rise to a doublet of doublets centered at 160.2 ppm with similar coupling constants, which could not be assigned without ambiguity. The IR spectrum of **6** features two modes for the asymmetric CO stretching vibration at 2055 and 2003 cm^{-1}, giving an average value of 2029 cm^{-1}. A small shoulder at 1968 cm^{-1} may be due to the presence of small amounts of the mixed $[LRh(CO)Cl]^+$ complex, which is not observed in solution. The $\vartheta_{avg,RhCO}$ value of **6** is considerably lower compared to that of the bis(phosphine) complex $[\{(R,R)\text{-}^{Ph}BPE\}Rh(CO)_2]BF_4$ (2070.5 cm^{-1}),[36] bis(NHC) complex $[\{(IBu))_2C_3H_5\}Rh(CO)_2]PF_6$ (2040 cm^{-1}),[37] and $[\{(S(IMe))_2CH_2\}Rh(CO)_2]PF_6$ (2045 cm^{-1})[27], which clearly underlines the strong donor properties of ligand **1**. This is in line with the average CO stretching frequency measured for $[(IDipPPh)RhCl(CO)_2]$ (2006 cm^{-1}), which showed that NHPs are a strongly donating ligand class, clearly outperforming NHCs.[4d]

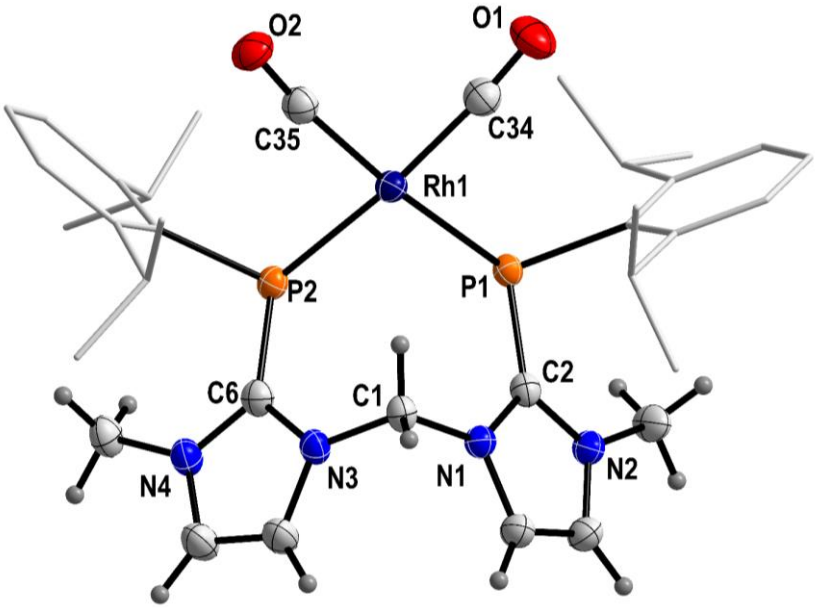

Figure 4. Solid-state structure of the cation in **6** with 50% probability thermal ellipsoids and the hydrogen atoms on the Dip substituents, which are rendered as wire-frame, omitted for clarity. Selected bond lengths [Å] and angles [°]: P1–C2 1.819(3), P2–C6 1.804(3), Rh1–P1 2.3742(6), Rh1–P2 2.3902(6), Rh1–C34 1.879(3), Rh1–C35 1.896(3); C34–Rh1–C35 88.45(11), C34–Rh1–P1 88.33(8), C35–Rh1–P1 171.37(8), C34–Rh1–P2 168.54(9), C35–Rh1–P2 90.97(8), P1–Rh1–P2 90.59(2), C2–P1–Rh1 114.75(8), C6–P2–Rh1 117.46(8).

Considering that there should be one additional lone pair of electrons available for coordination on each phosphorus atom in Rh-complex **4**, it was probed whether these could be engaged in the formation of bimetallic complexes. Thus, **4** was combined with $AuCl(SMe_2)$ in a 1:2 ratio in CH_2Cl_2, immediately affording a red precipitate (Scheme 8). After removal of the solvent and washing with *n*-hexane, the trimetallic complex [**1**·$(AuCl)_2$·Rh(cod)]Cl, **7**, was isolated in excellent yield. In solution, **7** is characterized by a doublet resonance in the $^{31}P\{^1H\}$ NMR spectrum at −50.7 ppm ($^1J_{Rh-P}$ = 124.9 Hz), considerably deshielded compared to complexes **4** and **6**, in agreement with both phosphorus lone pairs being engaged in coordination to Rh and Au. A single-crystal X-ray diffraction experiment confirmed the structure proposed for **7** (Figure 5), with the cod ligand attached to Rh, while each of the P atoms is now ligated by an additional AuCl fragment in a *trans*-geometry with respect to the rhodium metalacycle, giving a rare example of a trimetallic $RhAu_2$ complex. Liu and co-workers have recently introduced the class of AuPhos ligands, with the general formula $LAu-PR_2$ (L = NHC, R = H, Ad, Ph), which could further yield $(LAu)_2PiPr$ (Au_2Phos), of which the Rh(acac)CO complex was prepared and showed that Au_2Phos is a very electron-rich ligand.[38] Compared to the free ligand **1** and Rh complex **4**, the $P-C_{NHC}$ distances in **7** (1.836(7), 1.834(7) Å) are elongated, indicating considerably weakened $P-C_{NHC}$ double bond character, as expected if both lone pairs of electrons are engaged in metal coordination.

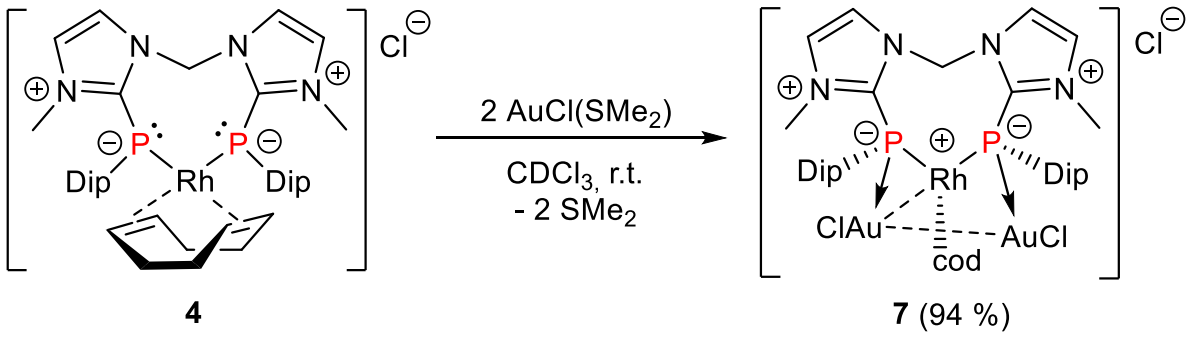

4 **7** (94 %)

Scheme 8. Synthesis of trimetallic complex **7**.

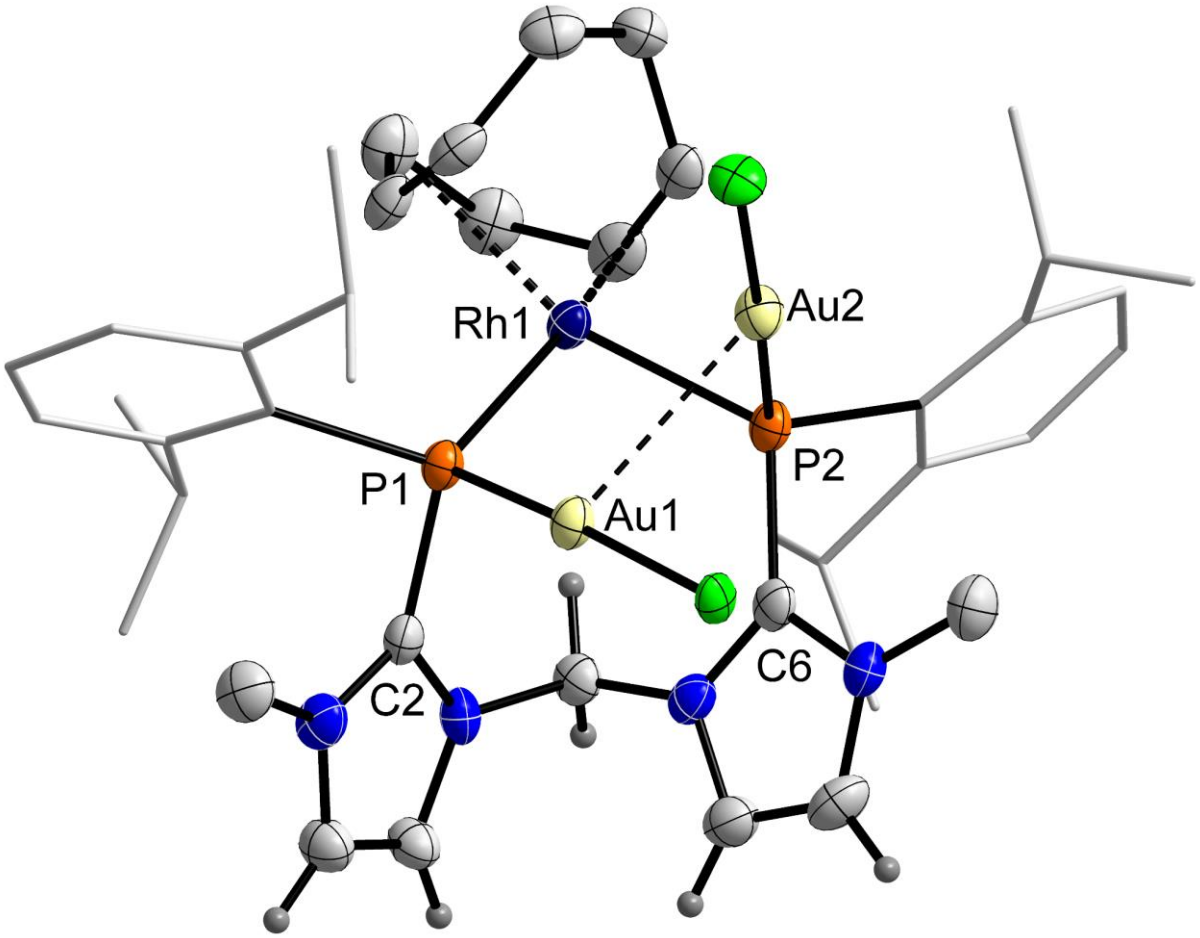

Figure 5. Solid-state structure of the cation in **7** with 50% probability thermal ellipsoids and the hydrogen atoms on the Dip substituents, which are rendered as wire-frame, omitted for clarity. Selected bond lengths [Å] and angles [°]: P1–C2 1.836(7), P2–C6 1.834(7), P1–Au1 2.2683(16), P2–Au2 2.2683(16), P1–Rh1 2.4214(16), P2–Rh1 2.3073(17), Au2–Rh1 3.0204(6), Rh1–H1B 2.7776(5); P1–Au1–Cl1 173.22(6), P1–Au1–Au2 86.86(4), P2–Au2–Cl2 173.86(7), P2–Rh1–P1 95.96(6), P2–Rh1–Au2 48.14(4), P1–Rh1–Au2 83.41(4), C2–P1–Au1 92.4(2), C2–P1–Rh1 123.0(2), Au1–P1–Rh1 108.77(6), C6–P2–Au2 109.6(2), C6–P2–Rh1 119.2(2), Au2–P2–Rh1 82.61(5).

The short Au···Au distance (2.9838(4) Å) indicates the presence of an aurophilic interaction through the **1**·Rh metallacycle,[39] which is in the same range as those measured in the complex $[Me_3PC(AuClPPh_2)_2]$[39b] (cf. Au···Au = 3.000(1) Å). The Rh–P distances (P1–Rh1 2.4214(16), P2–Rh1 2.3073(17) Å) vary considerably, as do the Rh–Au distances. A close contact is detected between Rh1 and Au2 (3.0204(6) Å), whereas the Rh1···Au1 distance (3.8137(6) Å) is considerably longer.

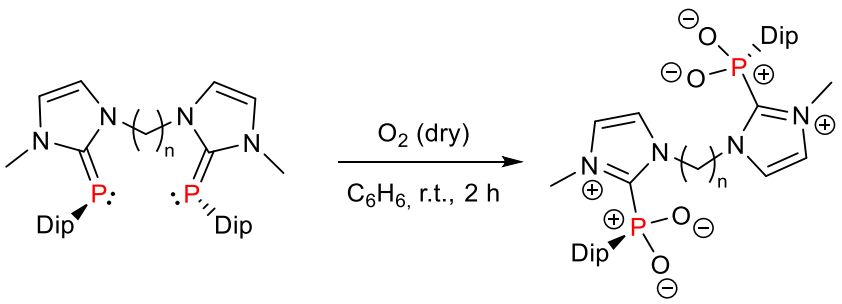

1 (n = 1)
2 (n = 3)

8 (n = 1, 48 %)
9 (n = 3, 94 %)

Scheme 9. Air oxidation of ligands **1** and **2**.

Exposing solutions of **4** in CH_2Cl_2 to air led to the clean formation of a new species within 72 h. A $^{31}P\{1H\}$ NMR singlet resonance at 4.7 ppm, corroborated with decolorization of the reaction solution, strongly suggested complex demetallation. In the solid state, **4** reacted only slowly with air, with incomplete conversion after 72 h. The nature of this decomposition product was ascertained by bubbling dry air through a C_6H_6 solution of ligand **1**, which resulted in the decolorization of the yellow solution to give a colorless precipitate, which was identified as the bis(NHC)-stabilized bis(dioxophosphorane) [(**1**)O_4], **8**, in 48 % yield. Additionally, **2** could be similarly converted to give [(**2**)O_4], **9**, in 94 % yield (Scheme 9), which displayed a diagnostic $^{31}P\{^1H\}$ NMR signal at 3.1 ppm, consistent with a C_{2h} symmetry in solution. X-ray quality crystals of **8** were grown by vapor diffusion of *n*-pentane into a saturated $CHCl_3$ solution. **8** crystallizes in the triclinic space group *P*-1 as a $CHCl_3$ solvate. With ca. 1.49 Å, the P–O distances (Figure 6) in the DipPO_2 moiety are in line with those measured in previously reported NHC-stabilized dioxophosphoranes (cf. (PhPO_2)IMe_4[40] 1.4902(10), 1.4855(11) Å) and other Lewis base stabilized dioxophospranes (cf. (^{Dip}TerPO_2)OPMe_3[41] 1.4641(19), 1.4721(17) Å; (PhPO_2)dmap[42] 1.4752(17), 1.4742(14)). Additionally, the P–C_{NHC} distances (1.8715(19), 1.8660(19) Å) increase significantly upon oxidation, compared to those observed in the free ligand **1** (cf. 1.773(3) Å).

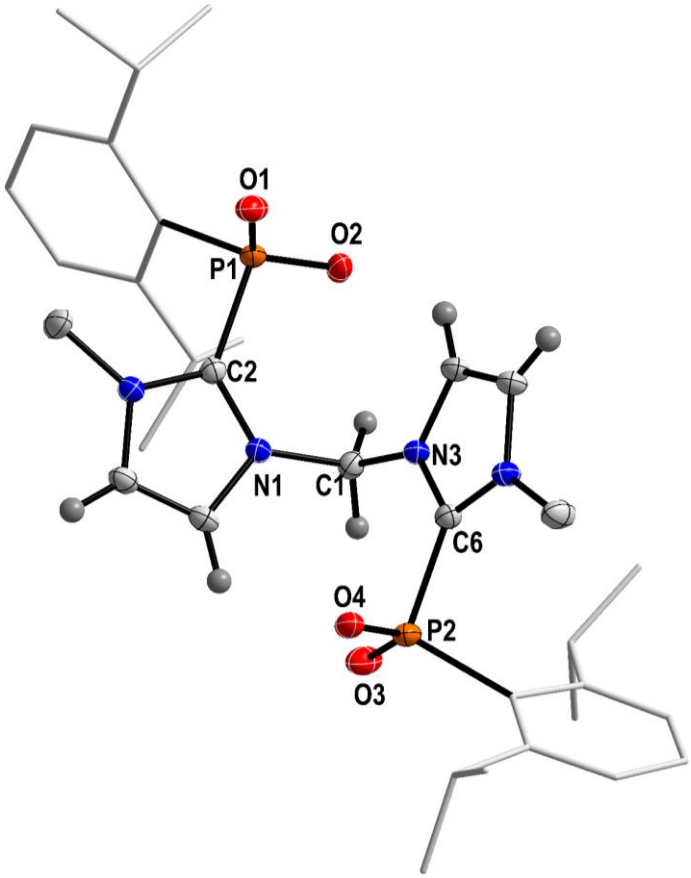

Figure 6. Solid-state structure of **8** with 30% probability thermal ellipsoids and the hydrogen atoms on the Dip substituents, which are rendered as wire-frame, omitted for clarity. Molecular structure of **8**. Selected bond lengths [Å] and angles [°]: P1–C2 1.8715(19), P1–O1 1.4860(16), P1–O2 1.4893(15), P2–C6 1.8660(19), P2–O3 1.4888(16), P2–O4 1.4943(16); O1–P1–O2 120.20(9), O1–P1–C2 101.12(9), O2–P1–C2 107.21(9), O3–P2–O4 119.10(9), O3–P2–C6 106.87(9), O4–P2–C6 100.70(8).

Conclusion

We report a novel route towards bis(NHP)s, by treating bis(NHC)s with triphosphirane Dip_3P_3 as a transfer reagent for the Dip–P moiety. This method provided access to methylene-bridged derivative **1** and propylene-bridged variant **2**. Bis(NHP) **1** proved to be a competent ligand, forming chelating, tetrahedral Fe(II) complex **3** and *cis*-chelating, square planar, cationic Rh(I) complex **4**, featuring COD still bound to Rh and an outer sphere chloride counter anion. While **4** is not a competent catalyst for the hydrogenation of the model substrates MAC and $ItMe_2$, analog **5** incorporating a BAr^F counteranion, was shown to catalyse the hydrogenation of both substrates under mild conditions at 1 mol% catalyst loading. Under a CO atmosphere, **4** was converted into

the cationic biscarbonyl complex **6**. Its average ν_{CO} stretching frequency of 2029 cm^{-1} indicated that the bis(NHP) ligand was a stronger electron donor than the corresponding bis(NHC)s or classical chelating diphosphines. The conversion of **1** to the heterotrimetallic complex **7**, featuring a central $RhAu_2$ core and significant Au···Au interactions, proved that both phosphorus lone pairs of each phosphorus atom can be involved in coordination. In addition, **1** and **2** could be cleanly converted to their corresponding bis-dioxophosphorane forms upon exposure to dry air, which have the potential to serve as hard, tetradentate oxygen ligands. We are currently investigating the potential to assemble other multimetallic complexes and probe the potential of complex **7** in dual catalysis, taking advantage of both Rh and Au. Moreover, we are looking into expanding the scope of this straightforward synthesis that generates chelating phosphorus ligands shown to be stronger electron donating than bis(phosphines) and bis(NHC)s, by introducing different linking groups between the NHCs, as well as testing other *cyclo*-oligophosphanes as P−R sources.

Acknowledgements

J.-E.S. wishes to thank the *Fonds der Chemischen Industrie* for financial support (Kekulé fellowship) and MITACS Canada for a Globalink Research Award. C. H.-J. and J.-E.S. thank the Leibniz Association for funding within the scope of the Leibniz ScienceCampus Phosphorus Research Rostock (www.sciencecampus-rostock.de). Financial support was provided by the Universities of Calgary and the Natural Sciences and Engineering Research Council of Canada (NSERC) in the form of Discovery Grant #2019-07195 to R.R.

Conflict of Interests

The authors declare no conflict of interest.

Keywords: Phosphorus • N-Heterocyclic Carbenes • Transition Metal Complexes • NHC Phosphinidene Adducts • Phosphaalkenes

References

[1] G. Frison, A. Sevin, *J. Organomet. Chem.* **2002**, *643-644*, 105-111.

[2] a) A. Doddi, M. Peters, M. Tamm, *Chem. Rev.* **2019**, *119*, 6994-7112; b) K. Schwedtmann, G. Zanoni, J. J. Weigand, *Chem. Asian J.* **2018**, *13*, 1388-1405; c) T. Krachko, J. C. Slootweg, *Eur. J. Inorg. Chem.* **2018**, *2018*, 2734-2754.

[3] L. Weber, *Eur. J. Inorg. Chem.* **2000**, *2000*, 2425-2441.

[4] a) M. Peters, A. Doddi, T. Bannenberg, M. Freytag, P. G. Jones, M. Tamm, *Inorg. Chem.* **2017**, *56*, 10785-10793; b) T. Krachko, M. Bispinghoff, A. M. Tondreau, D. Stein, M. Baker, A. W. Ehlers, J. C. Slootweg, H. Grützmacher, *Angew. Chem. Int. Ed.* **2017**, *56*, 7948-7951; c) M. Klein, G. Schnakenburg, A. Espinosa Ferao, N. Tokitoh, R. Streubel, *Eur. J. Inorg. Chem.* **2016**, *2016*, 685-690; d) D. Bockfeld, A. Doddi, P. G. Jones, M. Tamm, *Eur. J. Inorg. Chem.* **2016**, *2016*, 3704-3713; eV. A. K. Adiraju, M. Yousufuddin, H. V. Rasika Dias, *Dalton Trans.* **2015**, *44*, 4449-4454; fT. G. Larocque, G. G. Lavoie, *New J. Chem.* **2014**, *38*, 499-502.

[5] a) L. Werner, G. Horrer, M. Philipp, K. Lubitz, M. W. Kuntze-Fechner, U. Radius, *Z. Anorg. Allg. Chem.* **2021**, *647*, 881-895; b) H. Schneider, D. Schmidt, U. Radius, *Chem. Commun.* **2015**, *51*, 10138-10141.

[6] K. Pal, O. B. Hemming, B. M. Day, T. Pugh, D. J. Evans, R. A. Layfield, *Angew. Chem. Int. Ed.* **2016**, *55*, 1690-1693.

[7] I. A. J. Arduengo, D. H. V. Rasika, C. J. Calabrese, *Chem. Lett.* **1997**, *26*, 143-144.

[8] O. Back, M. Henry-Ellinger, C. D. Martin, D. Martin, G. Bertrand, *Angew. Chem. Int. Ed.* **2013**, *52*, 2939-2943.

[9] A. J. Arduengo, J. C. Calabrese, A. H. Cowley, H. V. R. Dias, J. R. Goerlich, W. J. Marshall, B. Riegel, *Inorg. Chem.* **1997**, *36*, 2151-2158.

[10] a) J.-E. Siewert, A. Schumann, C. Hering-Junghans, *Dalton Trans.* **2021**, *50*, 15111-15117; b) D. Dhara, P. Kalita, S. Mondal, R. S. Narayanan, K. R. Mote, V. Huch, M. Zimmer, C. B. Yildiz, D. Scheschkewitz, V. Chandrasekhar, A. Jana, *Chem. Sci.* **2018**, *9*, 4235-4243; c) N. Hayakawa, K. Sadamori, S. Tsujimoto, M. Hatanaka, T. Wakabayashi, T. Matsuo, *Angew. Chem. Int. Ed.* **2017**, *56*, 5765-5769.

[11] T. Wellnitz, C. Hering-Junghans, *Eur. J. Inorg. Chem.* **2021**, *2021*, 8-21.

[12] P. Gupta, J.-E. Siewert, T. Wellnitz, M. Fischer, W. Baumann, T. Beweries, C. Hering-Junghans, *Dalton Trans.* **2021**, *50*, 1838-1844.

[13] a) O. Lemp, C. von Hänisch, *Phosphorus Sulfur Silicon Relat. Elem.* **2016**, *191*, 659-661; b) M. Cicač-Hudi, J. Bender, S. H. Schlindwein, M. Bispinghoff, M. Nieger, H. Grützmacher, D. Gudat, *Eur. J. Inorg. Chem.* **2016**, *2016*, 649-658; c) M. Bispinghoff, H. Grützmacher, *Chimia* **2016**, *70*, 279; d) L. L. Liu, D. A. Ruiz, F. Dahcheh, G. Bertrand, *Chem. Commun.* **2015**, *51*, 12732-12735; e) A. Doddi, D. Bockfeld, T. Bannenberg, P. G. Jones, M. Tamm, *Angew. Chem. Int. Ed.* **2014**, *53*, 13568-13572; f) K. Hansen, T. Szilvási, B. Blom, S. Inoue, J. Epping, M. Driess, *J. Am. Chem. Soc.* **2013**, *135*, 11795-11798.

[14] T. J. Hadlington, A. Kostenko, M. Driess, *Chem. Eur. J.* **2021**, *27*, 2476-2482.

[15] R. Baierl, A. Kostenko, F. Hanusch, S. Inoue, *Dalton Trans.* **2021**, *50*, 14842-14848.

[16] R. Baierl, A. Kostenko, F. Hanusch, A. D. Beck, S. Inoue, *Eur. J. Org. Chem.* **2022**, *2022*, e202201072.

[17] W. Tang, X. Zhang, *Chem. Rev.* **2003**, *103*, 3029-3070.

[18] a) M. G. Gardiner, C. C. Ho, *Coord. Chem. Rev.* **2018**, *375*, 373-388; b) M. Poyatos, J. A. Mata, E. Peris, *Chem. Rev.* **2009**, *109*, 3677-3707.

[19] A. Schumann, F. Reiß, H. Jiao, J. Rabeah, J.-E. Siewert, I. Krummenacher, H. Braunschweig, C. Hering-Junghans, *Chem. Sci.* **2019**, *10*, 7859-7867.

[20] T. Scherg, S. K. Schneider, G. D. Frey, J. Schwarz, E. Herdtweck, W. A. Herrmann, *Synlett* **2006**, *2006*, 2894-2907.

[21] J. L. Anderson, R. Ding, A. Ellern, D. W. Armstrong, *J. Am. Chem. Soc.* **2005**, *127*, 593-604.

[22] A. K. Adhikari, T. Grell, P. Lönnecke, E. Hey-Hawkins, *Eur. J. Inorg. Chem.* **2016**, *2016*, 620-622.

[23] See Supporting Information for all experimental and computational details. CCDC 2265387-2265392 contain the crystallographic data for the structures reported in this paper. These can be obtained free of charge via www.ccdc.cam.ac.uk/data_request/cif.

[24] M. J. Burk, J. E. Feaster, R. L. Harlow, *Organometallics* **1990**, *9*, 2653-2655.

[25] B. D. Vineyard, W. S. Knowles, M. J. Sabacky, G. L. Bachman, D. J. Weinkauff, *J. Am. Chem. Soc.* **1977**, *99*, 5946-5952.

[26] L. Yang, D. R. Powell, R. P. Houser, *Dalton Trans.* **2007**, 955-964.

[27] I. R. Crossley, A. F. Hill, E. R. Humphrey, M. K. Smith, *Organometallics* **2006**, *25*, 2242-2247.

[28] M. Brookhart, M. L. H. Green, G. Parkin, *Proc. Natl. Acad. Sci.* **2007**, *104*, 6908-6914.

[29] M. Bortolin, U. E. Bucher, H. Ruegger, L. M. Venanzi, A. Albinati, F. Lianza, S. Trofimenko, *Organometallics* **1992**, *11*, 2514-2521.

[30] Y. Zhang, J. C. Lewis, R. G. Bergman, J. A. Ellman, E. Oldfield, *Organometallics* **2006**, *25*, 3515-3519.

[31] T. Lu, Q. Chen, *Chemistry–Methods* **2021**, *1*, 231-239.

[31] J. J. Race, A. L. Burnage, T. M. Boyd, A. Heyam, A. J. Martínez-Martínez, S. A. Macgregor, A. S. Weller, *Chem. Sci.* **2021**, *12*, 8832-8843.

[33] a) J.-O. Moritz, S. Chakrabortty, B. H. Müller, A. Spannenberg, P. C. J. Kamer, *J. Org. Chem.* **2020**, *85*, 14537-14544; b) C. R. Landis, J. Halpern, *J. Am. Chem. Soc.* **1987**, *109*, 1746-1754.

[34] a) E. Alberico, S. Möller, M. Horstmann, H.-J. Drexler, D. Heller, *Catalysts* **2019**, *9*, 582; b) A. Meißner, E. Alberico, H.-J. Drexler, W. Baumann, D. Heller, *Catal. Sci. Tech.* **2014**, *4*, 3409-3425; c) A. Preetz, C. Kohrt, A. Meißner, S. Wei, H.-J. Drexler, H. Buschmann, D. Heller, *Catal. Sci. Tech.* **2013**, *3*, 462-468.

[35] A. Preetz, H.-J. Drexler, C. Fischer, Z. Dai, A. Börner, W. Baumann, A. Spannenberg, R. Thede, D. Heller, *Chem. Eur. J.* **2008**, *14*, 1445-1451.

[36] D. Crozet, A. Gual, D. McKay, C. Dinoi, C. Godard, M. Urrutigoïty, J.-C. Daran, L. Maron, C. Claver, P. Kalck, *Chem. Eur. J.* **2012**, *18*, 7128-7140.

[37] J. A. Mata, A. R. Chianese, J. R. Miecznikowski, M. Poyatos, E. Peris, J. W. Faller, R. H. Crabtree, *Organometallics* **2004**, *23*, 1253-1263.

[38] R. Wei, S. Ju, L. L. Liu, *Angew. Chem. Int. Ed.* **2022**, *61*, e202205618.

[39] a) H. Schmidbaur, *Gold Bull.* **2000**, *33*, 3-10; b) H. Schmidbaur, W. Graf, G. Müller, *Angew. Chem. Int. Ed. Engl.* **1988**, *27*, 417-419.

[40] D. Bockfeld, T. Bannenberg, P. G. Jones, M. Tamm, *Eur. J. Inorg. Chem.* **2017**, *2017*, 3452-3458.

[41] F. Dankert, P. Gupta, T. Wellnitz, W. Baumann, C. Hering-Junghans, *Dalton Trans.* **2022**, *51*, 18642-18651.

[42] M. I. Arz, V. T. Annibale, N. L. Kelly, J. V. Hanna, I. Manners, *J. Am. Chem. Soc.* **2019**, *141*, 2894-2899.